社団法人 電子情報通信学会
THE INSTITUTE OF ELECTRONICS,
INFORMATION AND COMMUNICATION ENGINEERS

信学技報
TECHNICAL REPORT OF IEICE

MC-CDMA セルラ方式における下りリンクサイトダイバーシチの理論検討

アリ　アルニ† 井上　高道†　安達　文幸‡
東北大学大学院工学研究科電気・通信工学専攻　〒980-8579 仙台市青葉区荒巻字青葉 6-6-05
E-mail: †{arny,inoue}@mobile.ecei.tohoku.ac.jp, ‡adachi@ecei.tohoku.ac.jp

あらまし　セルラ方式では，セル境界のユーザは，受信信号レベルが弱いことと他セルからの大きな干渉を受けるために伝送特性が劣化する．これを解決するのがサイトダイバーシチである．また，アンテナダイバーシチを併用することによって，更に伝送特性を改善することができる．本論文では，MC-CDMA 下りリンクを対象に，自セル及び他セル干渉のガウス近似を用いて周波数選択性フェージング環境下の MC-CDMA 下りリンクの条件付 BER の理論式を導出している．また，モンテカルロ数値計算手法により平均 BER を求め，その累積分布からアウテージ確率を求め，下りリンク容量を求めている．理論計算結果と計算機シミュレーション結果とを比較し，理論検討の妥当性を確認している．

キーワード: *MC-CDMA*，サイトダイバーシチ，下りリンク容量，アウテージ確率，*MMSE- FDE*，アンテナダイバーシチ．

Theoretical Performance Analysis of Downlink Site Diversity in an MC-CDMA Cellular System

Arny ALI† Takamichi INOUE† Fumiyuki ADACHI‡
Department of Electrical and Communication Engineering, Graduate School of Engineering, Tohoku University
05 Aza-Aoba, Aramaki, Aoba-ku, Sendai, 980-8579 Japan
E-mail: †{arny,inoue}@mobile.ecei.tohoku.ac.jp, ‡adachi@ecei.tohoku.ac.jp

SUMMARY The downlink (base-to-mobile) bit error rate (BER) performance for a mobile user with relatively weak received signal in a multicarrier-CDMA (MC-CDMA) cellular system can be improved by utilizing the site diversity reception. With joint use of MMSE-based frequency domain equalization (FDE) and antenna diversity combining, the site diversity operation will increase the downlink capacity. In this paper, an expression for the theoretical conditional BER for the given set of channel gains is derived based on Gaussian approximation of the interference components. The local average BER is then obtained by averaging the conditional BER over the given set of channel gains using Monte-Carlo numerical method. The outage probability is measured from the numerically obtained cumulative distribution of the local average BER to determine the downlink capacity. Results from theoretical computation are compared to the results from computer simulation and discussed.

Keywords: *MC-CDMA, site diversity, downlink capacity, outage probability, MMSE-based FDE, antenna diversity.*

1. Introduction

Multicarrier-CDMA (MC-CDMA) has been considered as a wireless access candidate for a wideband downlink transmission due to its robustness against the frequency-selectivity of the multipath channel [1-2]. Moreover, the use of frequency-domain equalization (FDE) based on MMSE (minimum mean squared error), referred as MMSE-FDE, in wireless transmission has been shown to provide good bit error rate (BER) performance for an MC-CDMA system in a severe fading environment [2-3]. In a cellular system, MC-CDMA employs the single frequency reuse feature that efficiently utilizes the limited bandwidth, similar to a direct sequence CDMA (DS-CDMA) [4]. This feature initiates the use of site diversity reception, allowing a mobile user to receive signals from multiple base stations (BS's) and thus improving the downlink transmission performance for a mobile user with relatively weak received signal power, due to the shadowing loss and distance-dependent path loss. Recently, it has been shown by computer simulation in [5] that the site diversity operation can improve the downlink capacity with joint use of MMSE-FDE and receive antenna diversity. However, there has been no theoretical work to compare with the computer simulation results from [5]. The objective of this paper is to build the theoretical foundation to evaluate the downlink performance with site diversity operation and compare the theoretical performance results to the computer simulation results.

This paper is organized as follows. Sect. 2 presents the downlink site diversity reception and transmission system model for cellular MC-CDMA with MMSE-FDE and receive antenna diversity. The theoretical BER analysis is presented in Sect. 3, where expression for conditional BER is derived. This is followed by Sect. 4, where the local average BER is computed by averaging the conditional BER over the given set of channel gains using Monte-Carlo numerical method, and the numerically obtained cumulative distribution of the

local average BER is tabulated for finding the outage probability. Theoretical computation results are then compared to computer simulation results with discussion. Sect. 5 gives the conclusions for this paper and some future works.

2. System Model

2.1. Site diversity in downlink transmission

Assuming all BS's transmit pilot signals with equal power, a mobile user measures the average local received power from surrounding BS's and sorts them out in descending order. The "local average received power" means the instantaneous received power variations due to multipath fading is removed by taking the average so that only the effect of shadowing and distance-dependent path loss remains. In site diversity operation, the selection of active BS's is performed based on a threshold P_{th}. A BS having a local average received power within the threshold from the maximum will be selected as an active BS for the operation. Fig. 1 shows the site diversity operation model for the case of three (3) active BS's, with the radio network controller (RNC) monitoring the whole operation. The threshold P_{th} can control the number of active BS's and makes it an important design parameter in site diversity operation. When P_{th} is too small, the number of selected BS's is small and this decreases the downlink capacity. However, setting a too large P_{th} will result in selecting more BS's and increasing the interference power and for compensating this; the downlink capacity has to be reduced. Evidently, there shall be an optimum P_{th} that gives the maximum downlink capacity.

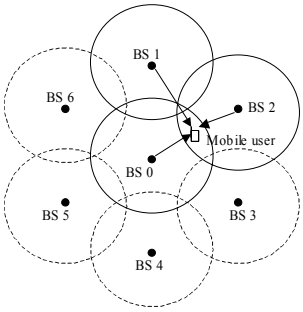

Fig. 1: Site diversity model.

2.2. Transmit/Receive Signal Representation

The downlink MC-CDMA transmitter/receiver systems for site diversity reception with joint use of MMSE-FDE and receive antenna diversity is illustrated in Fig. 2. A system with N_c subcarriers and spreading factor SF is assumed. At BS i, the data modulated symbol sequence $\{d_{u(j)}(n); n = 0 \sim N_c/SF - 1\}$ for user u of cell i is serial-to-parallel (S/P) converted into N_c/SF parallel data. Each of the S/P converter output is copied SF times and multiplied with the orthogonal spreading code $\{c_{u(j)}(k); k = 0 \sim SF - 1\}$. All users' spread signal components at each subcarrier are combined and multiplied with the common scrambling code $\{c_{PN(i)}(k); k = 0 \sim N_c - 1\}$ of BS i. Besides making the resultant signal to look like white-noise, different scrambling codes are used in different cell sites for separating cell sites. The composite transmit signal at subcarrier k is given as

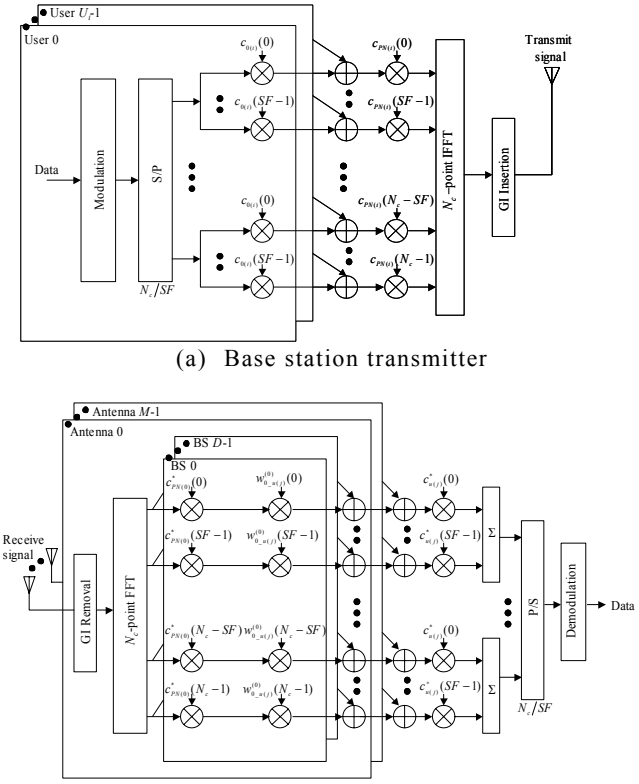

(a) Base station transmitter

(b) Mobile station receiver

Fig. 2: Downlink MC-CDMA system with site diversity reception

$$s_i(k) = \sqrt{\frac{2P_i}{SF}} \sum_{u(i)=0}^{U+\delta u_i - 1} d_{u(i)}\left(\left\lfloor \frac{k}{SF} \right\rfloor\right) c_{u(i)}(k \bmod SF) c_{PN(i)}(k) \quad (1)$$

with P_i and $U+\delta u_i$ defined as the transmit power and the number of active channels (users) per BS i, respectively; where δu_i denotes the number of additional channels necessary for BS i in site diversity operation; and $|d_{u(i)}(n)| = |c_{u(i)}(k)| = |c_{PN(i)}(k)| = 1$. The orthogonal spreading and the scrambling codes have the following characteristics

$$\begin{cases} \dfrac{1}{SF} \displaystyle\sum_{k=0}^{SF-1} c_{u(i)}(k) c^*_{u'(i)}(k) = \delta(u - u') \\ E\left[c_{PN(i)}(k) c_{PN(i)}(k')\right] = \delta(k - k') \end{cases} \quad .(2)$$

However, perfect orthogonality between users cannot be achieved in a multipath fading channel, and this produces the multiple access interference (MAI). Furthermore, the inter-cell interference (ICI) from other neighboring cells has to be considered since the scrambling codes between cells are not orthogonal. After N_c-point IFFT and cyclic N_g-sample guard interval (GI) insertion, the MC-CDMA transmit signal is then expressed as

$$s(t) = \sum_{k=0}^{N_c - 1} s_i(k) \exp\left(j 2\pi k \frac{t}{N_c}\right) \quad (3)$$

for $t=-N_g \sim N_c-1$. The signal is assumed to propagate through a frequency-selective block Rayleigh fading channel with L independent propagation paths. The MC-CDMA receive signal at antenna m of $u(j)$ equivalent baseband representation is given by

$$r_{u(j)}^{(m)}(t)=\sum_{i=0}^{\infty}\sum_{l=0}^{L-1}\xi_{i\_u(j),l}^{(m)}s_{i\_u(j)}(t-\tau_l)+n^{(m)}(t) \qquad (4)$$

for $t=-N_g \sim N_c-1$, where $n^{(m)}(t)$ is the zero-mean complex additive white Gaussian noise (AWGN) having a variance of $2N_0/T_c$ with N_0 being the single-sided power spectrum density. Both $\xi_{i\_u(j),l}^{(m)}$ and τ_l denote the complex channel gain and time delay of the path l transmitted from BS i and received by antenna m of user $u(j)$ in cell j, respectively. Uncorrelated fadings are assumed on each antenna. After the GI is removed, the received signal at each antenna is decomposed into N_c subcarrier components by N_c-point FFT processing. The kth subcarrier component is given as

$$R_{u(j)}^{(m)}(k)=\left[\sum_{i=0}^{\infty}H_{i\_u(j)}^{(m)}(k)\sqrt{\frac{2S_{i\_u(i)}}{SF}}\sum_{u(i)=0}^{U+\delta u_i-1}d_{u(i)}\left(\left\lfloor\frac{k}{SF}\right\rfloor\right)\right.$$
$$\left.\times c_{u(i)}(k \bmod SF)c_{PN(i)}(k)\right]+\Pi^{(m)}(k) \qquad ,(5)$$

where $S_{i\_u(j)}$ denotes the local average signal power received by user $u(j)$ from BS i, which is given by

$$S_{i\_u(j)}=P_{i\_u(j)}\times r_{i\_u(j)}^{-\alpha}\times 10^{-\beta(i)/10} \qquad (6)$$

with the distance between the BS i and user $u(j)$ given as $r_{i\_u(j)}$, the path loss exponent factor as α and the lognormal distributed shadowing loss standard deviation as β. The channel gain and the noise component due to AGWN for subcarrier k received at antenna m is given, respectively, as

$$\begin{cases}H_{i\_u(j)}^{(m)}(k)=\sum_{l=0}^{L-1}\xi_{i\_u(j),l}^{(m)}\exp\left(-j2\pi k\frac{\tau_l}{N_c}\right)\\ \Pi^{(m)}(k)=n^{(m)}(t)\exp\left(-j2\pi k\frac{t}{N_c}\right)\end{cases} \qquad .(7)$$

2.3. Joint MMSE-FDE and Receive Antenna Diversity

The N_c subcarrier components are multiplied by the complex conjugate of the scrambling code to extract the desired signal component from the selected active BS in the site diversity operation. To restore orthogonality between subcarriers, MMSE-FDE is performed. The weight for the joint MMSE-FDE and receive antenna diversity given by [5] is

$$w_{i\_u(j),MMSE}^{(m)}(k)=\frac{\Gamma_{i\_u(j),eff}H_{i\_u(j)}^{(m)*}(k)}{\sum_{i=0}^{\infty}\Gamma_{i\_u(j),eff}(U+\delta u_i)\sum_{m=0}^{M-1}\left|H_{i\_u(j)}^{(m)}(k)\right|^2+SF} \qquad (8)$$

with $\Gamma_{i\_u(j),eff}=\frac{E_s}{N_0}\times r_{i\_u(j)}^{-\alpha}\times 10^{-\beta(i)/10}$ and $E_s/N_0=P_{i\_u(j)}N_cT_c/N_0$ represents the ratio of effective symbol energy to the AWGN power spectrum density. Then, the signal components of each subcarrier k received by M antennas are all combined.

2.4. Decision Variable

To obtain the decision variable $y_{u(j)}(n)$ for the nth data modulated symbol of user $u(j)$, despreading is performed by multiplying SF soft samples $\{k=nSF \sim (n+1)SF-1; n=0 \sim N_c/SF-1\}$ of the combined subcarriers' components with the complex conjugate of the spreading code. The decision variable is given as

$$y_{u(j)}(n)=\frac{1}{SF}\sum_{k=nSF}^{(n+1)SF-1}\left(\sum_{m=0}^{M-1}\sum_{b=0}^{D-1}\varepsilon_b R_{i\_u(j)}^{(m)}(k)c_{PN(i)}^{*}(k)w_{i\_u(j)}^{(m)}(k)\right)$$
$$\times c_{u(j)}^{*}(k \bmod SF) \qquad ,(9)$$

where D is the allowable maximum number of active BS's and ε_b=1 (0) for the BS with $\Delta_b<P_{\text{th}}$ (otherwise) with Δ_b representing the difference of the local average received power from the maximum value. The active BS index is given in descending order and only D strongest BS's that satisfy $\Delta_b<P_{\text{th}}$ are selected for site diversity operation. After the parallel-to-serial (P/S) conversion, the set of N_c/SF decision variables is demodulated to recover the transmitted data symbol sequence. Substituting (5) into (9) gives

$$y_{u(i)}(n)=x_{u(i)}(n)+\mu_{noise}(n)+\mu_{MAI}(n)+\mu_{ICI}(n) \qquad ,(10)$$

where the first term represents the desired signal component, the second term the noise component due to AWGN, the third term the MAI and the fourth term the ICI.

3. BER Analysis

3.1. Derivation of SINR

It is understood from (10) that output of the despreader, $y_{u(j)}(n)$ is a random variable with mean $x_{u(j)}(n)$ conditioned on $H_{i\_u(j)}^{(m)}(k)$. The users' binary data, spreading codes and scrambling codes are assumed to be independently and identically distributed (i.i.d.) random variables taking values {+1,-1} with equal probability. Using the law of large numbers [6] for large U and SF, the MAI and ICI components can be approximated to be zero-mean complex-valued Gaussian noise. Consequently, the sum of $\mu_{noise}(n)$, $\mu_{MAI}(n)$ and $\mu_{ICI}(n)$ can be treated as a new zero-mean complex-valued Gaussian noise $\mu(n)$ [7]. The sum of the variances from the noise, MAI and ICI gives the

variance for $\mu(n)$, which is given by

$$2\sigma_{\mu}^{2}(n) = E\left[\left|\mu(n)\right|^{2}\right] = 2\sigma_{noise}^{2}(n) + 2\sigma_{MAI}^{2}(n) + 2\sigma_{ICI}^{2}(n) \quad .(11)$$

The conditional SINR (signal-to-interference plus noise power ratio) is then derived from the received signal components and given as

$$\gamma\left(E_s/N_0 \mid \left\{H_{i\_u(j)}^{(m)}(k)\right\}\right) = \frac{E\left[\left|x_{u(j)}(n)\right|^{2}\right]}{\sigma_{\mu}^{2}(n)}$$

$$= \frac{2\left(\frac{E_s}{N_0}\right)\left(\sum_{b=0}^{D-1}\sqrt{r_{b\_u(j)}^{-\alpha}\cdot 10^{-\beta(b)/10}}\cdot\frac{1}{SF}\sum_{k=nSF}^{(n+1)SF-1}\hat{H}_{b\_u(j)}(k)\right)^{2}}{\left[\frac{1}{SF}\sum_{k=nSF}^{(n+1)SF-1}\sum_{b=0}^{D-1}\sum_{m=0}^{M-1}\left|w_{b\_u(j)}^{(m)}(k)\right|^{2} + \frac{1}{SF}\frac{E_s}{N_0}\right.$$

$$\times\left(\begin{array}{l}\left(\sum_{b=0}^{D-1} r_{b\_u(j)}^{-\alpha}\times 10^{-\beta(b)/10}\times\left(U+\delta u_b-1\right)\right.\\ \left.\times\left\{\frac{1}{SF}\sum_{k=nSF}^{(n+1)SF-1}\left|\hat{H}_{b\_u(j)}(k)\right|^{2} - \left|\frac{1}{SF}\sum_{k=nSF}^{(n+1)SF-1}\hat{H}_{b\_u(j)}(k)\right|^{2}\right\}\right)\\ +\left(\begin{array}{l}\sum_{b=0}^{D-1}\sum_{\substack{i=0\\ i\neq b}}^{\infty} r_{i\_u(j)}^{-\alpha}\times 10^{-\beta(i)/10}\times\left(U+\delta u_i\right)\\ \times\frac{1}{SF}\sum_{k=nSF}^{(n+1)SF-1}\left|\sum_{m=0}^{M-1} w_{b\_u(j)}^{(m)}(k)H_{i\_u(j)}^{(m)}(k)\right|^{2}\end{array}\right)\end{array}\right] \quad .(12)$$

3.2. Expression for Conditional BER and Local Average BER

QPSK data modulation with all "1" transmission is considered. With the given set of channel gains $\left\{H_{i\_u(j)}^{(m)}(k); k=0\sim N_c-1; m=0\sim M-1; i=0\sim D-1\right\}$, the conditional BER can be expressed as

$$P_e\left(\gamma\left(E_s/N_0 \mid \left\{H_{i\_u(j)}^{(m)}(k)\right\}\right)\right) = \frac{1}{2}\Pr\left(\mathrm{Re}\left[y_{u(j)}(n)\right]<0 \mid \left\{H_{i\_u(j)}^{(m)}(k)\right\}\right) + \frac{1}{2}\Pr\left(\mathrm{Im}\left[y_{u(j)}(n)\right]<0 \mid \left\{H_{i\_u(j)}^{(m)}(k)\right\}\right)$$

$$= \frac{1}{2}erfc\left(\sqrt{\frac{\gamma\left(E_s/N_0 \mid H_{i\_u(j)}^{(m)}(k)\right)}{4}}\right) \quad (13)$$

where $erfc(x)$ is the complementary error function given by $erfc(x) = \frac{2}{\sqrt{\pi}}\int_{x}^{\infty}\exp(-t^{2})dt$. The theoretical local average BER for the transmitted nth modulated symbol can be numerically computed by averaging (13) over the given set of channel gains and written as

$$P_e\left(\frac{E_s}{N_0}\right) = \int_0^{\infty}\cdots\int_0^{\infty} P_e\left(\gamma\left(E_s/N_0 \mid \left\{H_{i\_u(j)}^{(m)}(k)\right\}\right)\right) p\left(\left\{H_{i\_u(j)}^{(m)}(k)\right\}\right)\prod_{m,k,i} dH_{i\_u(j)}^{(m)}(k) \quad (14)$$

where $p\left(\left\{H_{i\_u(j)}^{(m)}(k)\right\}\right)$ is the joint probability density function of $\left\{H_{i\_u(j)}^{(m)}(k)\right\}$. The averaging process is then performed by the Monte Carlo numerical method.

4. Numerical Results and Discussion

4.1. Monte-Carlo Process

The cellular structure and the computation condition are respectively shown in Table 1 and Fig. 3. In an interference-limited environment with negligible AWGN effect, each user will receive the dominant interference from the six adjacent cells' BS's. The user of interest is located in cell 0 and there are 18 surrounding cells considered as co-channel cells. The maximum number of active BS, D varies from 1 to 7 where D=1 corresponds to no site diversity operation and D=7 corresponds to site diversity operation with six adjacent co-channel cells.

In each Monte Carlo computation loop, the users' locations are randomly generated and followed by the generation of path and shadowing losses per user. For site diversity operation, active BS's for each user are selected based on P_{th}. The number of active channels for each BS is then determined. Next the set of fading channel gains and FDE weight for downlink transmission to user 0(0) are generated. Then the conditional SINR and BER are computed. The local average BER is tabulated with the locations for users randomly changed in every repeated computation loop. The outage probability (the probability of the local average BER larger than the required BER) is obtained using the cumulative distribution of the local average BER. Then, the maximum number U of users per cell that satisfies the allowable outage probability is determined as the downlink capacity.

Table 1: Computation Condition.

MC-CDMA	Data Modulation	QPSK
	Subcarrier number	N_c=256
	Spreading factor	SF=256
	Receive Antenna number	M=1~4
	FDE	MMSE
Site diversity	Required BER	10^{-2}
	Allowable outage probability	0.1
	Maximum active BS	D=1~7
	Threshold power	P_{th}=0~10 (dB)
Channel model	Path loss exponent factor	α= 3~4
	Shadowing loss standard deviation	β=4~10 (dB)
	Number of paths	L=16 Exponential Rayleigh fading
	Decay factor	γ=0~10 (dB)

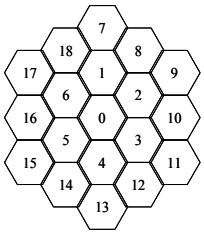

Fig. 3: Cellular Structure.

4.2. Numerical Results

4.2.1. Effect of site diversity threshold

The effect of site diversity threshold P_{th} on the downlink capacity, normalized by SF, is shown in Fig. 4. It is seen that the optimum P_{th} exists. As P_{th} increases from 0 dB to optimum, more active BS's are selected, and this gives better SINR and BER. Higher downlink capacity is thus obtained. However, as P_{th} becomes too large, the number of site diversity users is increased, creating excessive MAI and ICI. As a result, the downlink capacity is reduced. The optimum P_{th} becomes larger as path loss exponent factor α increases in both plots. This is because the received signal power decreases as α increases and causes the need for more active BS's in the site diversity operation. A fairly good agreement between the theoretical computation and computer simulation results are seen in Fig. 4.

4.2.2. Effects of path loss exponent factor α and shadowing loss standard deviation β

Figs. 5 and 6 show the effect of path loss exponent factor α and shadowing loss standard deviation β on the downlink capacity. For the case with site diversity opera, the optimum P_{th} is used, while P_{th}=0 (or D=1) for the case with no site diversity operation. In Fig. 5, the downlink capacity increases as α increases. Since path loss is proportional to the inverse α-th power of the distance, the interference power from relatively far BS's is greatly attenuated as α increases. This results in better SINR and thus, produces higher downlink capacity.

It is seen from Fig. 6 that the downlink capacity performance is almost unaffected by the increase of β in both cases. This is because as β increases, the variations in the interference power become larger and result in large interference, reducing the downlink capacity. However, since the interference power variations from different BS's are independent, the site diversity effect due to more active BS's selection increases and improves the received signal power. In both figures, theoretical computation result shows a fairly good agreement with the computer simulation result.

4.2.3. Effect of maximum number D of active BS's.

A maximum allowable active BS of D=7 has been assumed for active BS's selection in previous cases. The downlink capacity performance also depends on D. Fig. 7 shows that as D increases, the downlink capacity increases. However, since more additional channels are necessary for site diversity operation, the interference power increases and the downlink capacity is reduced. Thus, there is a maximum achievable downlink capacity for each D. Apparently, the maximum achievable value for different P_{th} lies in the region of D=3~7. Similar performance is seen for both theoretical computation and computer simulation plots. It is concluded that maximum achievable downlink capacity can be determined at D=3.

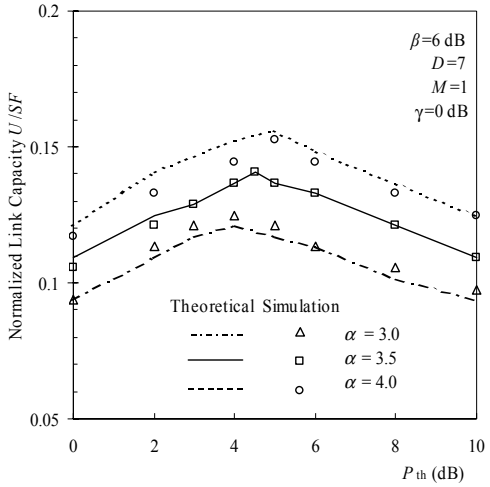

Fig. 4: Effect of site diversity threshold P_{th} on the downlink capacity.

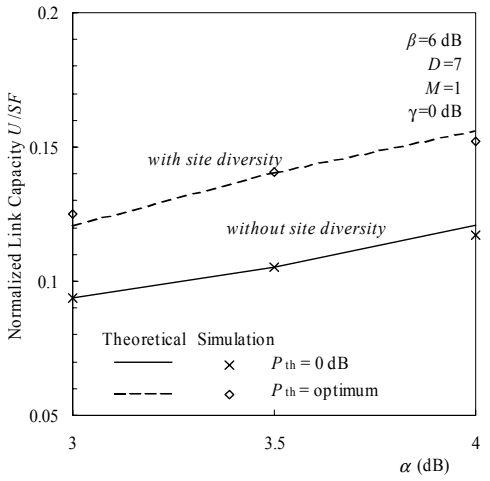

Fig. 5: Effect of path loss exponent factor α on the downlink capacity.

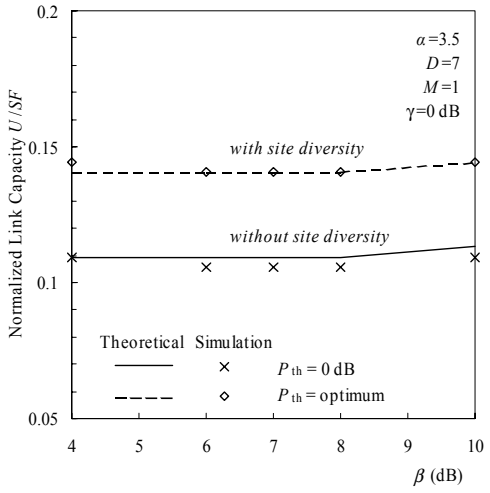

Fig. 6: Effect of shadowing loss standard deviation β on the downlink capacity.

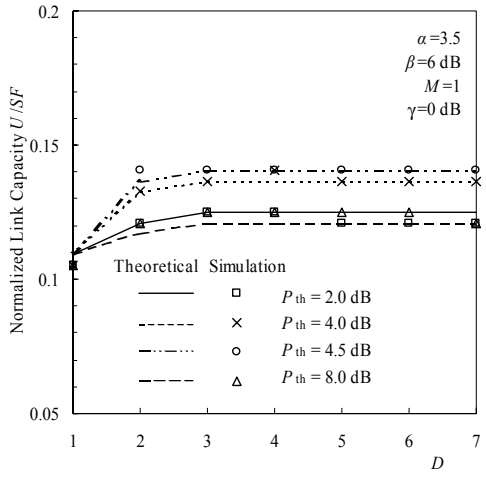

Fig. 7: Effect of maximum allowable number of D for active BS's on the downlink capacity.

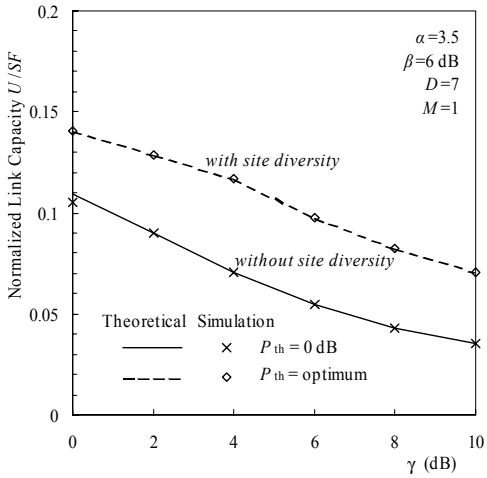

Fig. 8: Effect of decay factor, γ, on the downlink capacity.

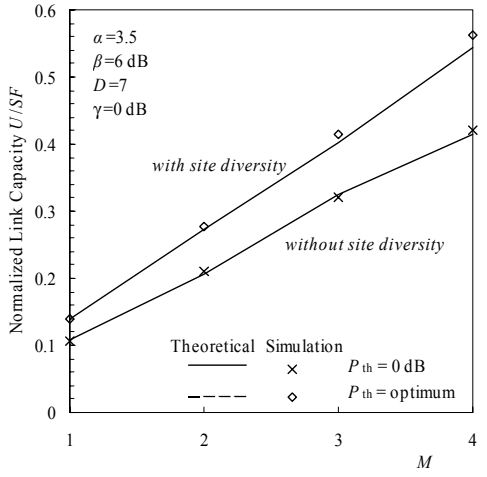

Fig. 9: Effect of number of receive antenna on the downlink capacity.

4.2.4. Effect of decay factor γ in exponential power delay profile cannel

The effect of decay factor γ of the exponential power delay profile channel is also examined. From Fig. 8, as γ increases, the frequency-selectivity of the channel becomes weaker, thus reducing the frequency-diversity effect in MC-CDMA. This degrades both SINR and BER, resulting in reduced downlink capacity performance. Similar results are shown for both theoretical computation and computer simulation plots.

4.2.5. Effect of number of receive antenna, *M*

Single antenna reception has been assumed in the previous cases. Fig. 9 shows downlink capacity improvement by employing the antenna diversity reception. The downlink capacity increases almost linearly with the number of M antennas, as shown both in theoretical computation and computer simulation plots.

5. Conclusions

In this paper, the theoretical treatment was developed for the downlink site diversity reception with joint use of MMSE-FDE and antenna diversity in an MC-CDMA cellular system. The theoretical expressions for the conditional SINR and BER were derived based on Gaussian approximation of the interference components; and the local average BER was numerically computed using Monte-Carlo method. The theoretical performance results were compared with computer simulation results to show a high degree of agreement. Evidently, from both theoretical and simulation evaluations, the site diversity operation improves the MC-CDMA downlink performance.

The theoretical analysis and computer simulation only considered the downlink case. Further works can include the studies on the uplink site diversity reception for MC-CDMA cellular system and finding ways to balance the optimum P_{th} and capacities for both link transmissions. Theoretical analyses on joint use with turbo-coded space-time transmit diversity (STTD) and fast TPC (transmit power control) can lead to a further interesting research.

References

[1] S. Hara and R. Prasad, "Overview of multicarrier CDMA," IEEE Commun. Magazine, vol. 35, no. 12, pp. 126-144, Dec. 1997.

[2] S. Hara and R. Prasad, "Design and performance of multicarrier CDMA system in frequency-selective Rayleigh fading channel," IEEE Trans. Vehicular Technology, vol. 48, pp. 1584-1595, Sept. 1999.

[3] N. Maeda, H. Atarashi, S. Abeta and M. Sawahashi, "Antenna diversity reception appropriate for MMSEC combining in frequency domain for forward link OFCDM packet wireless access," IEICE Trans. Commun., vol. E85-B, no. 10, pp. 1966-1977, Oct. 2002.

[4] A.J. Viterbi, CDMA: Principles of spread spectrum communications, Addison Wesley, 1995.

[5] T. Inoue, S. Takaoka and F. Adachi, "Frequency-domain equalization for MC-CDMA downlink site diversity and performance evaluation," IEICE Trans. Commun., vol. E88-B, no.1, Jan. 2005.

[6] J.G. Proakis, *Digital communications*, 4th. Ed., New York, McGraw Hill, 2000.

[7] F. Adachi and K. Takeda, "Bit error rate analysis of DS-CDMA with joint frequency-domain equalization and antenna diversity combining," IEICE Trans. Commun., vol. E87-B, no.10, pp. 2991-3002, Oct. 2004.